

Aberrant static and dynamic functional network connectivity in heart failure with preserved ejection fraction

Liang Jiang¹, Shenghua Liu¹, Lin Li², Wen Wu³, Zhongping Ai¹, Huiyou Chen¹, Xindao Yin^{1*} and Yu-Chen Chen^{1*}

¹Department of Radiology, Nanjing First Hospital, Nanjing Medical University, Nanjing, China; ²Department of Echocardiography, Nanjing First Hospital, Nanjing Medical University, Nanjing, China; and ³Department of Cardiology, Nanjing First Hospital, Nanjing Medical University, Nanjing, China

Abstract

Aims Heart failure may lead to brain functional alterations related to cognitive impairment. This study aimed to detect alterations of static functional network connectivity (FNC) and dynamic FNC in heart failure with preserved ejection fraction (HFpEF) and to estimate the association between the altered FNC and clinical features related to HFpEF.

Methods and results The clinical and resting-state functional magnetic resonance imaging (fMRI) data of HFpEF patients ($n = 35$) and healthy controls (HCs) ($n = 35$) were acquired at baseline. Resting-state networks (RSNs) were established based on independent component analysis (ICA) and FNC analyses were performed. The associations between the FNC abnormalities and clinical features related to HFpEF were analysed. Compared with HCs, HFpEF patients showed decreased functional connectivity within the default mode network, left frontoparietal network, and right frontoparietal network and increased functional connectivity within the right frontoparietal network and visual network. Negative correlations were observed between decreased dynamic FNC and the left ventricular end-diastolic diameter (LVDD) ($r = -0.435$, $P = 0.015$) as well as the left ventricular end-systolic diameter (LVDS) ($r = -0.443$, $P = 0.013$).

Conclusions The FNC disruption and altered temporal properties of functional dynamics in HFpEF patients may reflect the neural mechanisms of brain injury after HFpEF, which may deepen our understanding of the disease.

Keywords Heart failure; Functional network connectivity; Resting-state fMRI

Received: 23 July 2021; Revised: 28 March 2022; Accepted: 27 April 2022

*Correspondence to: Yu-Chen Chen, MD, PhD, and Xindao Yin, MD, PhD, Department of Radiology, Nanjing First Hospital, Nanjing Medical University, No. 68, Changle Road, Nanjing 210006, China. Tel: +862587726268; Fax: +862552236361. Email: chenychen1989@126.com and y.163yy@163.com

Liang Jiang and Shenghua Liu have contributed equally to this work.

Introduction

Heart failure (HF) is a rising global epidemic disease with relatively high mortality. Three main phenotypes describe HF according to measurement of the left ventricular (LV) ejection fraction (EF): HF with reduced EF (HFrEF), HF with preserved EF (HFpEF), and HF with mid-range EF. Almost half of HF patients are HFpEF, and the prevalence is increasing.¹ Cognitive decline in executive function, attention, episodic memory, language, psychomotor speed, and visuospatial ability is typical for patients with HF, with differences between HFrEF and HFpEF.² Neuroimaging research indicates that HF patients exhibit a diverse range of brain structural alterations and then

lead to cognitive impairment.^{3–5} Frey *et al.* recently found that reduced hippocampal volume observed at baseline was associated with impaired cognitive function in patients with predominantly mild HF.⁶ It is essential to determine the aberrant functional connectivity (FC) in HFpEF for understanding the ongoing injurious processes, which would help guide intervention strategies for neural protection in the condition.

Non-invasive magnetic resonance imaging (MRI) procedures have been implemented to evaluate brain alterations associated with HF. Recent works have shown alterations in several brain regions serving automatic, sensorimotor, mood, and cognition, including medial temporal lobes, cingulate gyrus, mammillary bodies, and fornix thalamus.^{7–9} Park *et al.*

found that the topology of functional integration and specialized characteristics in HF are significantly changed in regions showing altered FC, an outcome that would interfere with brain network organization.¹⁰ These prove that impaired resting-state functional organization may lead to temporal neuropsychologic and physiologic pathology in HF and may exacerbate the potential for further injury. However, the inter-network interactions in patients with HFpEF remain unclear in HF. In view of the ability to isolate various brain function networks, the independent component analysis (ICA) has been widely applied for identifying resting-state networks (RSNs) to define different remote interaction patterns.^{11,12} Meanwhile, the functional network connectivity (FNC) can represent the temporal correlation between these RSNs.¹³ Therefore, exploration of the RSNs and FNC may provide unique dysconnectivity information to understand the underlying neural mechanisms in patients with HFpEF.

In this study, we aimed to evaluate the whole brain network connectivity in patients with HFpEF using static FNC (sFNC) and dynamic FNC (dFNC) based on resting-state functional MRI (fMRI). Moreover, the associations between the altered FNC and clinical features related to HFpEF were analysed. This study will enable us to understand how HFpEF influences brain function connectivity change and provide some evidences of the neural mechanisms of brain injury after HFpEF.

Methods

Subjects and clinical data

Thirty-five patients with HFpEF and 35 age, gender, and body mass index (BMI) matched healthy controls (HCs) were prospectively enrolled between January 2016 and October 2019. HFpEF was diagnosed according to the European Society of Cardiology (ESC) guidelines for HF 2016.¹⁴ First, the patient should have symptoms and signs typical of HF. Second, echocardiography should show normal or only slightly reduced LVEF (reduced LVEF is defined as <50%). Finally, structural heart disease, such as LV hypertrophy and enlargement of the left atrium (LA), or direct and indirect measures of diastolic LV dysfunction, such as elevated E/e' or low e' or tricuspid regurgitation velocity, should be used.¹⁵ The patients were excluded if they met the following criteria: (i) diabetes mellitus, uncontrolled hypertension, significant valvular disease, previous myocardial infarction, and coronary revascularization; (ii) previous cardiac surgery; and (iii) estimated glomerular filtration rate < 30 mL/min. Besides, age and sex matched HCs were also recruited and met the following inclusion criteria: (i) without a history of heart disease, diabetes, hypertension, or dyslipidaemia; (ii) had normal exercise capacity by cardiopulmonary exercise testing; (iii) not on any

medications; (iv) normal resting echocardiograms and electrocardiograms; and (v) underwent the same neuroimaging tests as HFpEF patients. This study was approved by the Institutional Review Board of Nanjing Medical University. All participants provided written informed consent before undergoing MRI.

The demographic characteristics, systolic blood pressure (SBP), diastolic blood pressure (DBP), and relevant medical history were collected. Fasting plasma glucose, triglyceride, cholesterol, low-density lipoprotein, and high-density lipoprotein were derived from laboratory blood tests. LVEF, fractional shortening (FS), left ventricular end-diastolic diameter (LVDD), and left ventricular end-systolic diameter (LVDS) were derived from echocardiography. Diastolic dysfunction was assessed by the ratio of early diastolic mitral flow velocity and early diastolic myocardial velocity (E/Em ratio). LV mass was calculated by area-length method and indexed to body surface area (LVMI).

Cognitive function assessment

Mini-Mental State Examination (MMSE)¹⁶ and Montreal Cognitive Assessment (MoCA)¹⁷ were used to evaluate the neurocognitive state of all participants. MMSE was conducted prior to MoCA for each participant. Similar sections on 'Orientation' and 'Serial subtraction starting at 100' in both tests were tested only once and scored based on their response to the task in MMSE to avoid familiarization. The subjects with scores of ≥ 25 for MMSE or ≥ 26 were considered cognitively normal, and lower scores indicated poorer cognitive abilities.

Imaging procedure

Functional magnetic resonance imaging scan parameters

All participants completed fMRI scan on a 3.0 Tesla MRI scanner (Ingenia, Philips Medical Systems) using an eight-channel digital head coil receiver and parallel imaging technology. T1-weighted images of the whole brain were acquired for each subject with a three-dimensional turbo fast echo (3D-TFE) sequence with the following parameters: repetition time (TR): 8.1 ms; echo time (TE): 3.7 ms; slices: 170; thickness: 1 mm; gap: 0 mm; acquisition matrix: 256 × 256; flip angle (FA): 8°; and field of view (FOV): 256 mm × 256 mm. The structural sequence took 5 min and 28 s. The resting-state-fMRI (rs-fMRI) blood oxygen level-dependent (BOLD) scans were acquired axially using a gradient echo-planar imaging sequence with the following parameters: TR: 2000 ms; TE: 30 ms; slices: 36; gap: 0 mm; thickness: 4 mm; FOV: 240 mm × 240 mm; FA: 90°; and acquisition matrix: 64 × 64. The rs-fMRI sequence scan took 8 min and 6 s. During all resting-state scans, scanner noise and head motion were reduced by using earplugs and foam padding, and the

participants were instructed to close their eyes and rest peacefully.

Data preprocessing

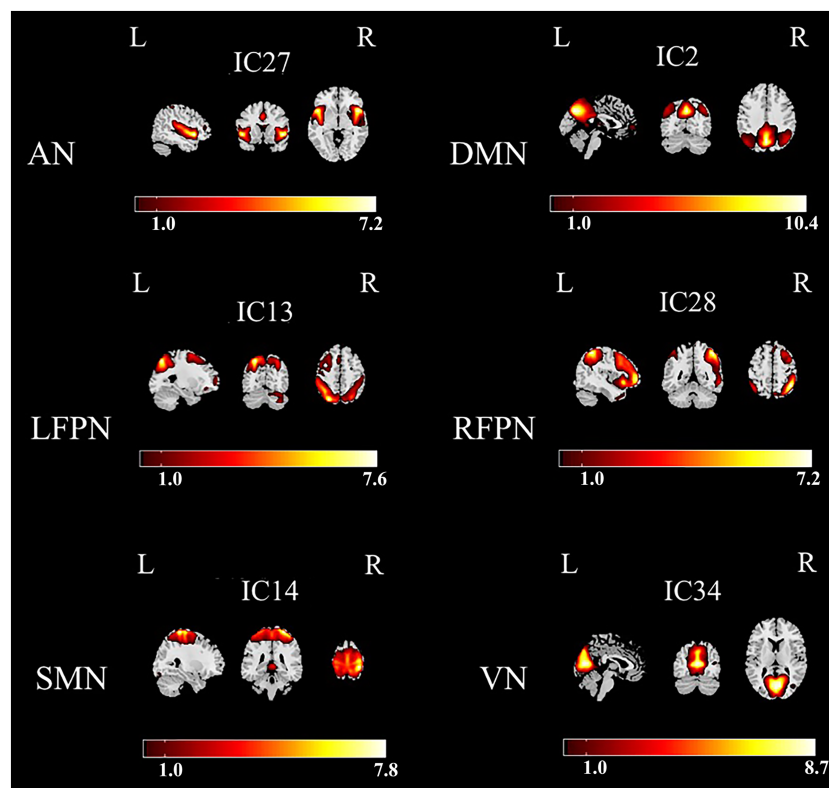
Data preprocessing was carried out using GRETNA software (<http://www.nitrc.org/projects/gretna>) implemented in MATLAB (Version R2013b), which included the following: (i) data format conversion (DICOM data transformed into NIFTI format); (ii) removal of volumes (the first 10 volumes were removed from each time series); (iii) slice-timing correction; (iv) realignment (head movement >2.0 mm translation or $>2.0^\circ$ rotation were excluded); (v) spatial normalization (warping individual T1 image to standard MNI space¹⁸); and (vi) spatial smoothing (a Gaussian smoothing kernel).

Resting-state networks selection and analysis

After data preprocessing, resting-state data of all participants were analysed using spatial ICA as implemented in the GIFT software (<http://mialab.mrn.org/software/gift/>) to select

RSNs. The number of independent components (ICs) was determined by using the minimum description length (MDL) criteria.¹⁹ First, a set of spatial ICA was executed on the aggregate data of the participants, resulting in an estimate of the ICs.²⁰ Then, the strength value of connectivity within each IC was converted into a z-score to reflect the degree of correlation between the time series of a given voxel and the average time series of its corresponding components. Among the 34 components resulting from ICA, six significant components were identified as RSNs through visual observation based on previous studies. These ICs were classified into six RSNs (Figure 1): attention network (AN), default mode network (DMN), left frontoparietal network (LFPN), right frontoparietal network (RFPN), sensorimotor network (SMN), and visual network (VN), which have been widely reported in previous resting-state fMRI research.^{21,22} For each RSN, the single-sample *t*-test was first used to obtain the z-maps for each group, the false discovery rate (FDR) was used to correct, and the statistical figure was obtained at the threshold of $P < 0.01$. Then, the two-sample *t*-test was used to compare the voxels within a union mask on the z-maps of the RSNs between-group. Between-group effects were thresholded at $P < 0.01$, corrected by FDR correction.

Figure 1 Functional relevant resting-state networks (RSNs). The spatial maps of six independent components (ICs) were selected as the RSNs for further analysis. AN, attention network; DMN, default mode network; LFPN, left frontoparietal network; RFPN, right frontoparietal network; SMN, sensorimotor network; VN, visual network.



Static functional network connectivity analysis between resting-state networks

First, a time-domain band-pass filter (band-pass 0.00–0.25 Hz) was used to reduce the influence of low-frequency drift and high-frequency physiological noise on the time process. Pearson correlation between any two RSN time processes for each participant was calculated to generate an FNC correlation matrix with the dimensions of 6 (ICs) \times 6. In the general linear model, FNC group difference estimation was performed for each pair of RSNs. The significance threshold was $P < 0.05$; FDR was used to correct for multiple comparisons.

Dynamic functional network connectivity analysis between resting-state networks

The temporal dFNC toolbox within the GIFT software was used for the analysis. The dFNC between ICA time courses was computed based on a sliding time-window approach.²³ We used a tapered window created by convolving a rectangle (width = 30 s, 15 TRs) with a Gaussian ($\sigma = 3$ TRs) and advancing 1 TR at each step.²⁴ A *k*-means algorithm with the squared Euclidean distance, 500 iterates, and 150 replicates dFNC windows were partitioned into four clusters.²⁵ The number of states was determined using the elbow criterion (the ratio of within-cluster distance to between-clusters distances). The connectivity pattern of each subject for each state was estimated as a subject median of the subject windows that were assigned to this state. Using subject state vectors, we also computed the percentage of occurrence of each dFNC state for each subject. The group difference was computed using two-sample *t*-tests at each state and results were corrected for multiple comparisons using the FDR ($P < 0.05$).

Statistical analysis

Demographic and clinical characteristic were analysed using commercially available software (SPSS for Windows, Version 19.0; SPSS). Continuous data are shown as the mean \pm SD, whereas categorical variables are presented as absolute and relative frequencies. The differences between HFpEF patients and HCs were assessed using the χ^2 test for categorical variables and an independent-samples *t*-test or Fisher's exact test for continuous variables. $P < 0.05$ was considered to indicate statistical significance. For FNC analysis, group comparisons between HFpEF and HC groups were performed using two-sample *t*-tests. Pearson's correlation coefficients between dFNC values and echocardiographic parameters, dFNC values, and cognitive scores were analysed with a significance level of $P < 0.05$.

Results

Participants and clinical data

Among 70 participants in the study, four patients were excluded due to excessive head motion artefacts after the fMRI data head motion check. Thirty-one HFpEF patients [17 men and 14 women; mean age (years \pm SD) 59.39 \pm 6.51; range, 47–69] and 35 subjects [22 men and 13 women; mean age (years \pm SD) 56.77 \pm 6.25; range, 43–70] were analysed. The education, MMSE scores, and MoCA scores were not significantly different between HFpEF groups and HC groups. The high-density lipoprotein in HFpEF groups was significantly lower than that in HC groups (1.06 \pm 0.23, 1.34 \pm 0.42; $t = 3.205$, $P = 0.002$); the other laboratory blood tests (fasting plasma glucose, triglyceride, cholesterol, low-density lipoprotein, SBP, and DBP) were not significantly different in two groups. Echocardiography examination was performed in patients with HFpEF. In HFpEF group, LVEF was (61.19 \pm 5.33)%; FS was (33.48 \pm 3.36)%; LVDd was (47.48 \pm 4.36) mm; and LVDs was (30.97 \pm 3.89) mm (Table 1). There were no significant differences of echocardiography information between HFpEF group and HCs. The HFpEF patients had higher E/Em ratio and LVMI than the HCs (Table 1).

Independent component analysis and component selection

A total of 34 ICs were extracted by ICA, among which 6 components were selected as the RSNs for further analysis. Six networks with these components were labelled as follows (Figure 1): The attention network (AN) (IC27) mainly included the dorsal anterior cingulate and anterior insular cortices, as well as part of the prefrontal areas. The default mode network (DMN) (IC2) included the posterior cingulate cortex, inferior parietal, and medial prefrontal cortex nodes. The left frontoparietal network (LFPN) (IC13) included the inferior parietal lobule, superior parietal lobule, and temporal lobule. The right frontoparietal network (RFPN) (IC28) included the left middle frontal gyrus, inferior parietal lobule, superior parietal lobule, and angular gyrus. The sensorimotor network (SMN) (IC14) was mainly focused at the bilateral primary somatosensory cortex, including precentral and postcentral gyri areas. The visual network (VN) (IC34) included the primary visual cortex [the bilateral calcarine sulcus and medial extrastriate region (e.g. the lingual gyrus and cuneus)].

Group functional connectivity differences within resting-state networks

The FC analysis showed four RSNs had significant differences between HFpEF and HC groups, including the DMN, LFPN,

Table 1 Demographic clinical characteristic in patients with HFpEF and HCs

Characteristics	HCs (n = 35)	HFpEF (n = 31)	t/χ^2 value	P value
Age (years)	56.77 ± 6.25	59.39 ± 6.51	-1.664	0.101
Gender (male/female)	22/13	17/14	0.437	0.618
Education	11.91 ± 2.42	11.87 ± 2.32	0.074	0.941
MMSE	29.03 ± 1.22	28.68 ± 1.08	1.230	0.223
MoCA	27.66 ± 1.55	26.87 ± 1.73	1.948	0.056
Fasting plasma glucose (mmol/L)	5.17 ± 0.32	5.35 ± 0.93	-1.055	0.296
Triglyceride (mmol/L)	1.71 ± 1.38	1.70 ± 1.10	0.048	0.962
Cholesterol (mmol/L)	4.71 ± 1.06	4.19 ± 1.43	1.689	0.096
LDL (mmol/L)	2.84 ± 0.93	2.41 ± 1.01	1.836	0.071
HDL (mmol/L)	1.34 ± 0.42	1.06 ± 0.23	3.205	0.002*
SBP (mmHg)	129.74 ± 10.46	127.61 ± 11.18	0.799	0.427
DBP (mmHg)	80.89 ± 6.97	79.55 ± 8.61	0.697	0.488
LVEF	63.34 ± 5.98	61.19 ± 5.33	1.604	0.113
FS (%)	34.51 ± 2.86	33.48 ± 3.36	1.420	0.160
LVDd (mm)	48.40 ± 3.47	47.48 ± 4.36	0.974	0.333
LVDs (mm)	31.20 ± 3.10	30.97 ± 3.89	0.349	0.728
E/Em	8.57 ± 2.03	15.87 ± 1.57	-16.183	<0.001**
LVMI (g/m ²)	101.77 ± 12.06	135.55 ± 13.01	-10.945	<0.001**

Note: Data are the mean ± standard deviation.

Abbreviations: DBP, diastolic blood pressure; E/Em, the ratio of early diastolic mitral flow velocity and early diastolic myocardial velocity; FS, fractional shortening; HCs, healthy controls; HDL, high-density lipoprotein; HFpEF, heart failure with preserved ejection fraction; LDL, low-density lipoprotein; LVDd, left ventricular end-diastolic diameter; LVDs, left ventricular end-systolic diameter; LVEF, left ventricular ejection fraction; LVMI, left ventricular mass index; MMSE, Mini-Mental State Examination; MoCA, Montreal Cognitive Assessment; SBP, systolic blood pressure.

* $P < 0.05$.

** $P < 0.001$.

RFPN, and VN (Table 2 and Figure 2). Compared with the HC group, the HFpEF group exhibited decreased FC within the DMN (right inferior frontal operculum), LFPN (left superior frontal lobe), and RFPN (right medial superior frontal lobe and right middle frontal lobe). Moreover, there was increased FC in the RFPN (left superior frontal lobe) and VN (right superior occipital lobe) in the HFpEF group compared with the HC group. Based on voxel-wise analysis, the resting-state FC did not show significant alteration in AN and SMN.

Group differences in static functional network connectivity

For the sFNC analysis, six networks were analysed between HFpEF group and HC group. Relative to the HC group, the HFpEF group exhibited significantly decreased negative network interactions between DMN and AN.

Group differences in dynamic functional network connectivity

Time-varying FNC over the scan duration can be represented by five states. FNC states are characterized by the cluster centroids (Supporting Information, Figure S1). Significant differences between groups in dFNC were observed only in State 3 (16% dFNC) (Supporting Information, Figure S2). Clustering results with $k = 5$ are shown in Figure 3A. Reoccurrence fraction in State 3 (0.08 ± 0.09 vs. 0.23 ± 0.17) and mean dwell time in State 3 (7.32 ± 5.91 vs. 13.78 ± 9.34) in HFpEF group were significantly shorter than those in HC group ($t = 4.329$, $P < 0.001$; $t = 3.305$, $P = 0.002$) (Figure 3B,C) (Supporting Information, Table S1). Group differences in dFNC using the window width of 40, 50, and 60 s corresponding to 20 TRs, 25 TRs, and 30 TRs, respectively, were also shown in the Supporting Information, Figures S3–S5.

Table 2 Brain regions with significant differences connectivity within resting-state networks between heart failure with preserved ejection fraction patients and healthy controls

	Brain regions	BA	Peak MNI coordinates x, y, z (mm)	Peak T value	Voxels
DMN	Frontal_Inf_Oper_R	25	51, 12, 27	3.8335	55
LFPN	Frontal_Sup_L	10	-21, 57, 3	3.6666	41
RFPN	Frontal_Sup_Medial_R	17	9, 39, 42	5.0615	153
	Frontal_Sup_L	6	-21, 33, 36	-4.1927	80
	Frontal_Mid_R	33	48, 42, 12	4.3437	150
VN	Occipital_Sup_R	23	18, -90, 18	-3.8723	56

Abbreviations: DMN, default mode network; Frontal_Inf_Oper_R, right inferior frontal operculum; Frontal_Sup_L, left superior frontal lobe; Frontal_Sup_Medial_R, right medial superior frontal lobe; LFPN, left frontoparietal network; Occipital_Sup_R, right superior occipital lobe; RFPN, right frontoparietal network; VN, visual network.

Figure 2 Group functional connectivity (FC) differences within resting-state networks (RSNs). Significant differences between the HFpEF and HC groups were found within four RSNs. DMN, default mode network; Frontal_Inf_Oper_R, right inferior frontal operculum; Frontal_Sup_L, left superior frontal lobe; Frontal_Sup_Medial_R, right medial superior frontal lobe; LFPN, left frontoparietal network; Occipital_Sup_R, right superior occipital lobe; RFPN, right frontoparietal network; VN, visual network.

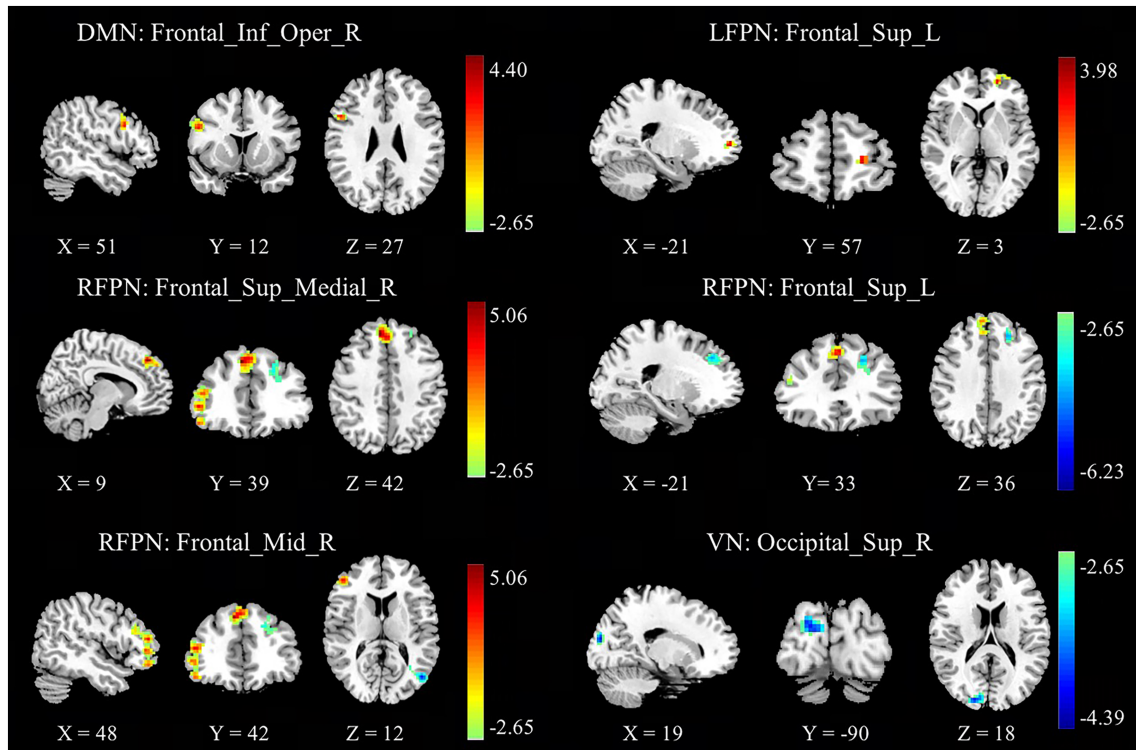
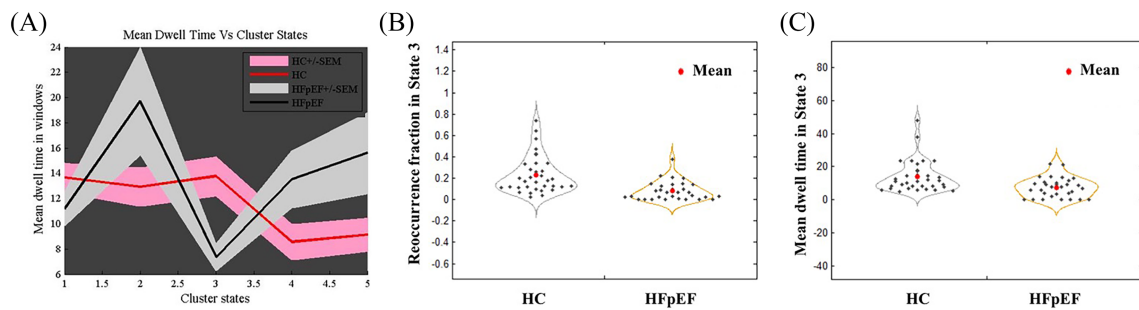


Figure 3 (A) Mean dwell time in windows vs. cluster states between HC and HFpEF; (B) recurrence fraction in State 3 and (C) mean dwell time in State 3 between HC and HFpEF were plotted using violin plots. HC, healthy controls; HFpEF, heart failure with preserved ejection fraction.

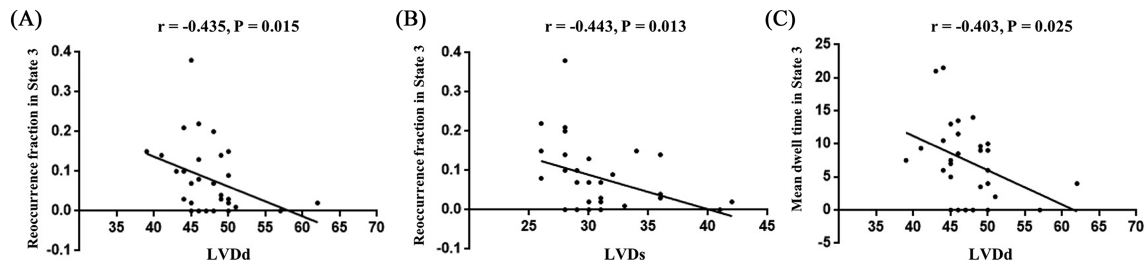


Correlation analysis

Correlations were performed between the dFNC and echocardiographic parameters, dFNC, and cognitive scores (Supporting Information, Table S2). The significant negative

correlations were found between recurrence fraction in State 3 and LVDd ($r = -0.435, P = 0.015$) (Figure 4A) and recurrence fraction in State 3 and LVDs ($r = -0.443, P = 0.013$) (Figure 4B). In addition, a significant negative correlation was found between the mean dwell time in State 3 and LVDd ($r = -0.403, P = 0.025$) (Figure 4C). However, we did not find any significant correlations between the dFNC

Figure 4 (A) The significant negative correlations were found between recurrence fraction in State 3 and LVDD ($r = -0.435$, $P = 0.015$), (B) recurrence fraction in State 3 and LVDs ($r = -0.443$, $P = 0.013$), and (C) mean dwell time in State 3 and LVDD ($r = -0.403$, $P = 0.025$). LVDD, left ventricular end-diastolic diameter; LVDs, left ventricular end-systolic diameter.



values and the E/Em ratio and LVMI ($P > 0.05$). Moreover, there were no significant correlations between dFNC values and cognitive scores.

Discussion

Previous studies have indicated that cognitive impairment is highly prevalent in patients with HF using the neuropsychological assessment, with deficits being most prominent in the domains of executive function, memory, language, and mental speed.^{26,27} Frey *et al.* found that patients with HF showed more advanced medial temporal lobe atrophy compared with controls, and the degree of medial temporal lobe atrophy was strongly associated with the severity of cognitive impairment.⁵ Others studies have also reported that patients with HF have brain changes related to cognitive function.^{6,14} However, the samples of these studies were heterogeneity. It is unclear whether the subtypes of HF (HFpEF) will cause brain changes. In our study, we found decreased FC within LFPN, RFPN, and DMN and increased FC within RFPN and VN in HFpEF. Park *et al.* demonstrated that HF patients had aberrant spontaneous functional connections in various brain areas using rs-fMRI, which were related to sensorimotor, autonomic, mood, and cognitive regulation.¹⁰ DMN is widely known to be associated with cognitive and emotional processing,²⁸ and FPN is critical for the ability to coordinate behaviour in a rapid, accurate, and flexible goal-driven manner.²⁹

Heart failure patients had tissue injury in most of brain regions (including hippocampus, anterior thalamus, fornix, mammillary bodies, caudate nuclei, putamen, cerebellum, and frontal cortices) that regulate cognitive, behavioural, and planning functions.³⁰ In this study, we found that the decreased FC was mainly in right inferior frontal operculum, left superior frontal lobe, right medial superior frontal lobe, and right middle frontal lobe in patients with HFpEF. The frontal lobes have progressively acquired a central role in most aspects of cognition and behaviour. In addition, the RFPN (left

superior frontal lobe) and VN (right superior occipital lobe) showed increase in patients with HFpEF. The FPN is pivotal in visual-spatial attention and motor function. The VN is associated with the processing of visual information. Given all this, the results of the increased RFPN and VN may suggest a compensatory mechanism to lessen the consequences of nerve damage caused by DMN and FPN and help maintain the patient's cognitive abilities.

It is worth pointing out that the HFpEF group exhibited significantly decreased negative interactions between DMN and AN, which was an important finding that had not been previously reported in HFpEF. The DMN is responsible for control and integration of primary perception and advanced cognition.³¹ The decline in attention and reduction in volume of the attention-related cortex reflects the impaired function of AN.³² Athilingam *et al.* showed that HFpEF patients had delayed recall and reduced abstraction abilities scored by MoCA.³³ Therefore, we believed that the changes in the interactions between DMN and AN may provide further information on how HFpEF patients can adjust the connectivity of the related networks during cognitive tests.

The dFNC could capture uncontrolled but reoccurring patterns of interactions among intrinsic networks during task engagement or at rest, which has not been explored in HFpEF patients. The five reoccurring dFNC states, significantly different from static connectivity, suggest the human brain is highly dynamic.²³ Our results showed that HFpEF patients demonstrated shorter time in State 3, including the recurrence fraction and dwell time, which had negative correlations with LVDD and LVDs. The mechanism proposed for brain injury in HF is multifactorial. The cerebral blood flow, the neurohormonal axis, and the inflammatory axis in HF were thought to have a role in the interaction between HF, cognition, and structural brain changes.³⁴ A possible explanation of our results might be found in the complex interaction between the LVDD and LVDs in the HFpEF patients and its effect on the recurrence fraction and mean dwell time in State 3. The correspondence between changes in LVDD and LVDs and changes in dFNC suggest that variability in the recurrence fraction and mean dwell time in State 3 may contribute from

fluctuations in autonomic tone and their potential psychological correlates. In addition, the window size from 30 s to 1 min had relatively little impact on dynamics.

There are several limitations and shortcomings in the present work that have to be considered. First, this is a preliminary cross-sectional study of FNC changes in HFpEF with limited sample size, so that it is difficult to direct the casual relationship between brain functional network and HFpEF. More longitudinal studies with larger samples are needed. Second, other brain networks may play an important role in the pathophysiology of brain injury in HFpEF, and detecting the variation of the FC and FNC in multiple networks will provide insight into the neural mechanism in depth. Finally, the ICA method cannot reveal the directionality of the interactions between networks. Further studies are required to assess the specific and directional function in coupling with other brain networks in HFpEF.

Conclusions

To summarize, this is the first study to assess function connectivity and the FNC properties in HFpEF. Our findings demonstrated that decreased negative network interactions between DMN and AN in sFNC and shorter dwelling time and reoccurrence fraction in dFNC and decreased dwelling time and reoccurrence fraction in dFNC were associated with LVDD and LVDs in HFpEF. We believe these findings could potentially help our understanding of the neural mechanisms of brain injury after HFpEF.

Conflict of interest

The authors declare that there is no potential conflict of interests regarding the publication of this paper.

Funding

None.

References

1. Dunlay SM, Roger VL, Redfield MM. Epidemiology of heart failure with preserved ejection fraction. *Nat Rev Cardiol.* 2017; **14**: 591–602.
2. Alwerdt J, Edwards JD, Athilingam P, O'Connor ML, Valdés EG. Longitudinal differences in cognitive functioning among older adults with and without heart failure. *J Aging Health.* 2013; **25**: 1358–1377.
3. Alosco ML, Hayes SM. Structural brain alterations in heart failure: a review of the literature and implications for risk of Alzheimer's disease. *Heart Fail Rev.* 2015; **20**: 561–571.
4. Song R, Xu H, Dintica CS, Pan KY, Qi X, Buchman AS, Bennett DA, Xu W. Associations between cardiovascular risk,

Supporting information

Additional supporting information may be found online in the Supporting Information section at the end of the article.

Figure S1. States 1-5 functional network connectivity (FNC) matrices. Positive correlations are in the yellow to red range, while negative correlations are light to dark blue.

Figure S2. Significant differences between HC and HFpEF group were observed in State 3.

Figure S3. dFNC analysis between RSNs using a tapered window created by convolving a rectangle (width = 40s, 20TRs). (A-B) Time-varying FNC over the scan duration can be represented by 5 States. Significant differences between groups in dFNC were observed only in State 3. (C) Reoccurrence fraction in State 3 (0.07 ± 0.09 vs 0.23 ± 0.18) and Mean dwell time in State 3 (7.48 ± 7.06 vs 15.77 ± 10.32) in HFpEF group were significant shorter than those in HC group ($t=4.462$, $P<0.001$; $t=3.762$, $P<0.001$).

Figure S4. dFNC analysis between RSNs using a tapered window created by convolving a rectangle (width = 50s, 25TRs). (A-B) Time-varying FNC over the scan duration can be represented by 5 States. Significant differences between groups in dFNC were observed only in State 3. (C) Reoccurrence fraction in State 3 (0.19 ± 0.16 vs 0.35 ± 0.25) and Mean dwell time in State 3 (14.84 ± 12.56 vs 29.61 ± 36.17) in HFpEF group were significant shorter than those in HC group ($t=3.133$, $P=0.003$; $t=2.266$, $P=0.029$).

Figure S5. dFNC analysis between RSNs using a tapered window created by convolving a rectangle (width = 60s, 30TRs). (A-B) Time-varying FNC over the scan duration can be represented by 5 States. Significant differences between groups in dFNC were observed only in State 5. (C) Reoccurrence fraction in State 5 (0.10 ± 0.13 vs 0.30 ± 0.27) and Mean dwell time in State 3 (8.23 ± 10.51 vs 25.35 ± 24.04) in HFpEF group were significant shorter than those in HC group ($t=4.008$, $P<0.001$; $t=3.820$, $P<0.001$).

Table S1. Demographic clinical characteristic in patients with HFpEF and HCs.

Table S2. Correlations analysis between the dFNC and echocardiographic parameters and cognitive scores in HFpEF patients.

- structural brain changes, and cognitive decline. *J Am Coll Cardiol*. 2020; **75**: 2525–2534.
5. Frey A, Sell R, Homola GA, Malsch C, Kraft P, Gunreben I, Morbach C, Alkonyi B, Schmid E, Colonna I, Hofer E, Müllges W, Ertl G, Heuschmann P, Solymosi L, Schmidt R, Störk S, Stoll G. Cognitive deficits and related brain lesions in patients with chronic heart failure. *JACC Heart Fail*. 2018; **6**: 583–592.
 6. Frey A, Homola GA, Henneges C, Mühlbauer L, Sell R, Kraft P, Franke M, Morbach C, Vogt M, Müllges W, Ertl G, Solymosi L, Pirpamer L, Schmidt R, Pham M, Störk S, Stoll G. Temporal changes in total and hippocampal brain volume and cognitive function in patients with chronic heart failure—the COGNITION.MATTERS-HF cohort study. *Eur Heart J*. 2021; **42**: 1569–1578.
 7. Pan A, Kumar R, Macey PM, Fonarow GC, Harper RM, Woo MA. Visual assessment of brain magnetic resonance imaging detects injury to cognitive regulatory sites in patients with heart failure. *J Card Fail*. 2013; **19**: 94–100.
 8. Almeida OP, Garrido GJ, Etherton-Beer C, Lautenschlager NT, Arnolda L, Alfonso H, Flicker L. Brain and mood changes over 2 years in healthy controls and adults with heart failure and ischaemic heart disease. *Eur J Heart Fail*. 2013; **15**: 850–858.
 9. Almeida OP, Garrido GJ, Beer C, Lautenschlager NT, Arnolda L, Flicker L. Cognitive and brain changes associated with ischaemic heart disease and heart failure. *Eur Heart J*. 2012; **33**: 1769–1776.
 10. Park B, Roy B, Woo MA, Palomares JA, Fonarow GC, Harper RM, Kumar R. Lateralized resting-state functional brain network organization changes in heart failure. *PLoS ONE*. 2016; **11**: e0155894.
 11. De Luca M, Beckmann CF, De Stefano N, Matthews PM, Smith SM. fMRI resting state networks define distinct modes of long-distance interactions in the human brain. *Neuroimage*. 2006; **29**: 1359–1367.
 12. Fox MD, Raichle ME. Spontaneous fluctuations in brain activity observed with functional magnetic resonance imaging. *Nat Rev Neurosci*. 2007; **8**: 700–711.
 13. Qin Y, Li Y, Sun B, He H, Peng R, Zhang T, Li J, Luo C, Sun C, Yao D. Functional connectivity alterations in children with spastic and dyskinetic cerebral palsy. *Neural Plast*. 2018; **2018**: 7058953.
 14. Ponikowski P, Voors AA, Anker SD, Bueno H, Cleland JG, Coats AJ, Falk V, González-Juanatey JR, Harjola VP, Jankowska EA, Jessup M, Linde C, Nihoyannopoulos P, Parissis JT, Pieske B, Riley JP, Rosano GM, Ruilope LM, Ruschitzka F, Rutten FH, van der Meer P. 2016 ESC Guidelines for the diagnosis and treatment of acute and chronic heart failure: the Task Force for the diagnosis and treatment of acute and chronic heart failure of the European Society of Cardiology (ESC). Developed with the special contribution of the Heart Failure Association (HFA) of the ESC. *Eur J Heart Fail*. 2016; **18**: 891–975.
 15. Donal E, Lund LH, Oger E, Hage C, Persson H, Reynaud A, Ennezat PV, Bauer F, Sportouch-Dukhan C, Drouet E, Daubert JC, Linde C. Baseline characteristics of patients with heart failure and preserved ejection fraction included in the Karolinska Rennes (KaRen) study. *Arch Cardiovasc Dis*. 2014; **107**: 112–121.
 16. Feng L, Chong MS, Lim WS, Ng TP. The Modified Mini-Mental State Examination test: normative data for Singapore Chinese older adults and its performance in detecting early cognitive impairment. *Singapore Med J*. 2012; **53**: 458–462.
 17. Dong Y, Sharma VK, Chan BP, Venketasubramanian N, Teoh HL, Seet RC, Tanicala S, Chan YH, Chen C. The Montreal Cognitive Assessment (MoCA) is superior to the Mini-Mental State Examination (MMSE) for the detection of vascular cognitive impairment after acute stroke. *J Neurol Sci*. 2010; **299**: 15–18.
 18. Ashburner J, Friston KJ. Unified segmentation. *Neuroimage*. 2005; **26**: 839–851.
 19. Li YO, Adali T, Calhoun VD. Estimating the number of independent components for functional magnetic resonance imaging data. *Hum Brain Mapp*. 2007; **28**: 1251–1266.
 20. Calhoun VD, Adali T, Pearlson GD, Pekar JJ. A method for making group inferences from functional MRI data using independent component analysis. *Hum Brain Mapp*. 2001; **14**: 140–151.
 21. Wang C, Cai H, Sun X, Si L, Zhang M, Xu Y, Qian Y. Large-scale internetwork functional connectivity mediates the relationship between serum triglyceride and working memory in young adulthood. *Neural Plast*. 2020; **2020**: 8894868.
 22. Jiang SF, Shi JY, Yang ZT, Zhang L, Chen HJ. Aberrant dynamic functional network connectivity in cirrhotic patients without overt hepatic encephalopathy. *Eur J Radiol*. 2020; **132**: 109324.
 23. Damaraju E, Allen EA, Belger A, Ford JM, McEwen S, Mathalon DH, Mueller BA, Pearlson GD, Potkin SG, Preda A, Turner JA, Vaidya JG, van Erp TG, Calhoun VD. Dynamic functional connectivity analysis reveals transient states of dysconnectivity in schizophrenia. *Neuroimage Clin*. 2014; **5**: 298–308.
 24. Du Y, Pearlson GD, Yu Q, He H, Lin D, Sui J, Wu L, Calhoun VD. Interaction among subsystems within default mode network diminished in schizophrenia patients: a dynamic connectivity approach. *Schizophr Res*. 2016; **170**: 55–65.
 25. Malhi GS, Das P, Outhred T, Bryant RA, Calhoun V. Resting-state neural network disturbances that underpin the emergence of emotional symptoms in adolescent girls: resting-state fMRI study. *Br J Psychiatry*. 2019; **215**: 545–551.
 26. Vogels RL, Oosterman JM, van Harten B, Scheltens P, van der Flier WM, Schroeder-Tanka JM, Weinstein HC. Profile of cognitive impairment in chronic heart failure. *J Am Geriatr Soc*. 2007; **55**: 1764–1770.
 27. Malik AS, Giamouzis G, Georgiopolou VV, Fike LV, Kalogeropoulos AP, Norton CR, Sorescu D, Azim S, Laskar SR, Smith AL, Dunbar SB, Butler J. Patient perception versus medical record entry of health-related conditions among patients with heart failure. *Am J Cardiol*. 2011; **107**: 569–572.
 28. Mantini D, Vanduffel W. Emerging roles of the brain's default network. *Neuroscientist*. 2013; **19**: 76–87.
 29. Marek S, Dosenbach NUF. The frontoparietal network: function, electrophysiology, and importance of individual precision mapping. *Dialogues Clin Neurosci*. 2018; **20**: 133–140.
 30. Woo MA, Kumar R, Macey PM, Fonarow GC, Harper RM. Brain injury in autonomic, emotional, and cognitive regulatory areas in patients with heart failure. *J Card Fail*. 2009; **15**: 214–223.
 31. Zhao Z, Wu J, Fan M, Yin D, Tang C, Gong J, Xu G, Gao X, Yu Q, Yang H, Sun L, Jia J. Altered intra- and inter-network functional coupling of resting-state networks associated with motor dysfunction in stroke. *Hum Brain Mapp*. 2018; **39**: 3388–3397.
 32. Cardin V. Effects of aging and adult-onset hearing loss on cortical auditory regions. *Front Neurosci*. 2016; **10**: 199.
 33. Athilingam P, D'Aouf RF, Miller L, Chen L. Cognitive profile in persons with systolic and diastolic heart failure. *Congest Heart Fail*. 2013; **19**: 44–50.
 34. Havakuk O, King KS, Grazette L, Yoon AJ, Fong M, Bregman N, Elkayam U, Kloner RA. Heart failure-induced brain injury. *J Am Coll Cardiol*. 2017; **69**: 1609–1616.